EARTH SURFACE PROCESSES AND LANDFORMS, VOL 22, 849–868 (1997)

# RATES AND PROCESSES OF PERIGLACIAL SOLIFLUCTION: AN EXPERIMENTAL APPROACH

CHARLES HARRIS[1*], MICHAEL C. R. DAVIES[2] AND JEAN-PIERRE COUTARD[3]

[1]*Department of Earth Sciences, University of Wales Cardiff, PO Box 914, Cardiff, CF1 3YE, UK*
[2]*Department of Civil Engineering, University of Dundee, Dundee DD1 4HN, UK*
[3]*Centre de Geomorphologie du CNRS, 24 Rue des Tilleuls, F-14000 Caen, France*

*Received 21 May 1996; Revised 20 October 1996; Accepted 30 December 1996*

## ABSTRACT

Cold room physical modelling of periglacial solifluction processes on an experimental slope of 12° is described, and data on soil temperatures, surface frost heave, thaw consolidation, downslope soil movement and porewater pressures over seven freeze–thaw cycles are presented. These data are analyzed in the context of laboratory determination of the rheometry of the experimental soils at high moisture contents. It is concluded that the observed thaw-induced solifluction represents pre-failure soil shear strain and results from loss of strength due to the combined effects of raised porewater pressures during thaw consolidation and upward seepage pressures as water flows towards the surface away from the thaw front. An investigation of the rheometry of thawing soils offers the prospect of an analytical model to predict rates and depths of periglacial solifluction. © 1997 by John Wiley & Sons, Ltd.

*Earth surf. process. landforms*, **22,** 849–868 (1997)
No. of figures: 15 No. of tables: 2 No. of refs: 37
KEY WORDS: periglacial; solifluction; physical modelling

## INTRODUCTION

The thaw consolidation theory (Morgenstern and Nixon, 1971) may be applied to an appropriate slope model to provide an analytical framework for the prediction of rapid slope failures during seasonal thawing of periglacial slopes. However, it is usually the case that the thaw consolidation ratio remains below its critical value for slope failure, so that shallow landsliding in most periglacial environments is infrequent and occurs only in response to particularly favourable environmental conditions (Lewkowicz, 1992). Most periglacial slopes are, however, characterized by solifluction, the slow downslope flow of saturated soil that occurs during the summer thaw period. Solifluction may therefore be regarded as pre-failure strain in the thawing soil (Harris *et al.* 1995). Currently there is no analytical approach available to predict its rate and duration. The ultimate aim of the present research project is to develop an analytical model to enable such predictions to be made.

This paper presents results of laboratory simulation of periglacial solifluction processes in non-cohesive soils. Previous experiments (Coutard *et al.*, 1988; Harris, 1993; Harris *et al.*, 1993), have demonstrated the advantages of controlled laboratory simulation in the investigation of periglacial slope processes. During the present work, an experimental slope formed of two different soils was subjected to seven cycles of downward freezing and thawing. Soil temperatures, porewater pressures and slope movements were monitored at half-hourly intervals using a PC logging system. The experimental design has been described in detail by Harris *et al*. (1996) and results of porewater pressure measurements during soil thawing and their analysis in the context of slope stability are discussed in Harris *et al*. (1995). Here we present data on frost heave and downslope soil displacements and discuss factors influencing movement rates and mechanisms. In addition, data are presented on the rheology of the two experimental soils in relation to moisture contents, providing an empirical basis for future predictive analytical techniques.

* Correspondence to: C. Harris
Contract grant sponsor: NERC; contract grant number: GR9/1089

CCC 0197-9337/97/090849–20 $17.50 

## PROCESS STUDIES

Measurements of periglacial solifluction, particularly surface rates, have been reported from a wide range of periglacial environments (e.g. Harris, 1981, 1987; Lewkowicz, 1988; Frenzel, 1993), but field studies of soil movement mechanisms and their controlling factors are rare. Washburn (1967), Benedict (1970), Harris (1972, 1977) and Smith (1988) have emphasized the importance of both frost heave during soil freezing and soil moisture contents during soil thawing in determining rates of solifluction, while field monitoring by Matsuoka (1994) has demonstrated a strong relationship between soil displacements and frost heave where frost creep is dominant. A 20 year data set from Spitsbergen was used by Åkerman (1993) to explore the relationships between solifluction rates and environmental factors. Relationships with climatic parameters were found to be complex and the most significant non-climatic factors were soil granulometry and moisture content, both of which significantly influence frost heave.

Laboratory simulation experiments allow boundary conditions to be defined and environmental factors to be controlled, hence facilitating the investigation of process variables. One of the earliest such studies was that by Higashi and Corte (1971), who demonstrated the role of needle-ice formation in near-surface frost creep. Coutard *et al*. (1988) and Harris *et al*. (1993) explored the influence of soil granulometry on solifluction rates, demonstrating strong relationships between soil granulometry, moisture content, frost heave and downslope displacement.

Mechanisms of solifluction have been inferred from field observations, and the importance of slow flow of saturated soil has been emphasized since Andersson's original definition of the term 'solifluction' in 1906 (e.g. Permafrost Subcommittee, National Research Council of Canada, 1988). The relative importance of gelifluction and frost creep has been extensively discussed (Taber, 1943; Sigafoos and Hopkins, 1952; Williams, 1957; Jahn, 1961; Washburn, 1967; French 1976; Harris 1981). Laboratory experiments using soils with differing granulometry allowed Harris *et al*. (1993) to demonstrate that the ratio of gelifluction to frost creep in four experimental soils increased dramatically as silt contents increased and sand contents decreased.

Micromorphological investigations by Van Vliet-Lanoë *et al*. (1984) revealed the existence of microshears within soils subjected to frost creep on an experimental slope. Micromorphological evidence has been further utilized by Van Vliet-Lanoë (1985a,b) to argue that slow frost creep is not associated with rotation of sand grains and cryogenic peds within the soil, but that gelifluction (saturated flow) does cause such rotation, leading to rounding of peds and the development of matrix coatings on sand grains. Bertran (1993), however, stressed that flat, disc-shaped clasts do not undergo rotation during solifluction, and concluded therefore that there is no simple relationship between microstructure and the type of movement (frost creep or solifluction).

## EXPERIMENTAL DESIGN AND INSTRUMENTATION

A slope of gradient 12° comprising two natural soil strips each 2 m wide, 0·3 m thick and 5 m long was constructed within a refrigerated 5 m × 5 m tank (Figures 1 and 2). The vertical boundary between the two adjacent soils was lined with a double layer of polythene lubricated with silicon oil. A similar double polythene layer was placed along the sides of the experimental slope. Hence, boundary friction was minimized, and no lateral seepage of water between the adjacent soil slope members was possible.

The basal sand layer was connected to an external water supply, so that soil freezing took place in an open hydraulic system. The air temperature above the slope was lowered to approximately –10°C during freezing. Thawing took place at ambient laboratory temperatures, which ranged from +9°C in cycle 2 (winter) to +15°C in cycle 4 (summer). The adjacent soil strips forming the experimental slope comprised natural soils collected from quarry faces in Normandy, France. The soil from Vire was derived from Precambrian slate and consisted of a sandy silt (Table I), while that from Feuguerolles was derived from Ordovician mudstone and comprised a poorly sorted gravelly sandy silt. Selected geotechnical parameters are given in Table I and compared with data from field studies of periglacial solifluction processes. It can be seen that the experimental soils provide good analogues for many arctic and alpine solifluction soils.

Instrumentation included semiconductor temperature sensors and thermistor arrays to monitor soil temperatures, Druck miniature pore pressure transducers filled with antifreeze to monitor porewater pressures,

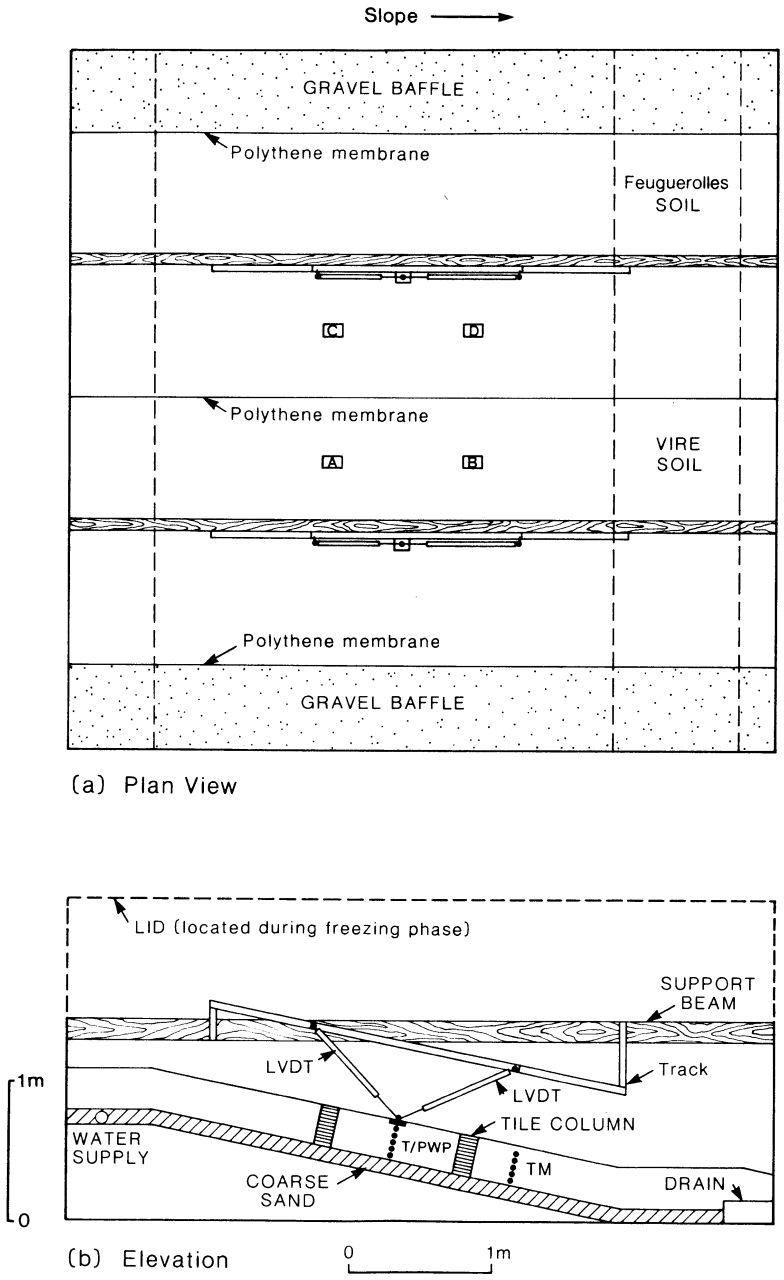


Figure 1. Diagram of experimental slope: (a) plan, (b) section. Tile columns are labelled A–D. TM, thermistors; T, semiconductor temperature sensors; PWP, porewater pressure transducers.

and linear voltage displacement transformers (LVDTs) to monitor frost heave and downslope soil displacement (Harris *et al.*, 1996). Instruments were scanned at half-hourly intervals using a PC-controlled data logging system. The LVDTs were arranged in pairs above each soil strip in the form of fixed-base triangles mounted on slotted tracks. The apex of each LVDT triangle consisted of a perspex footplate with 20 mm long anchor points

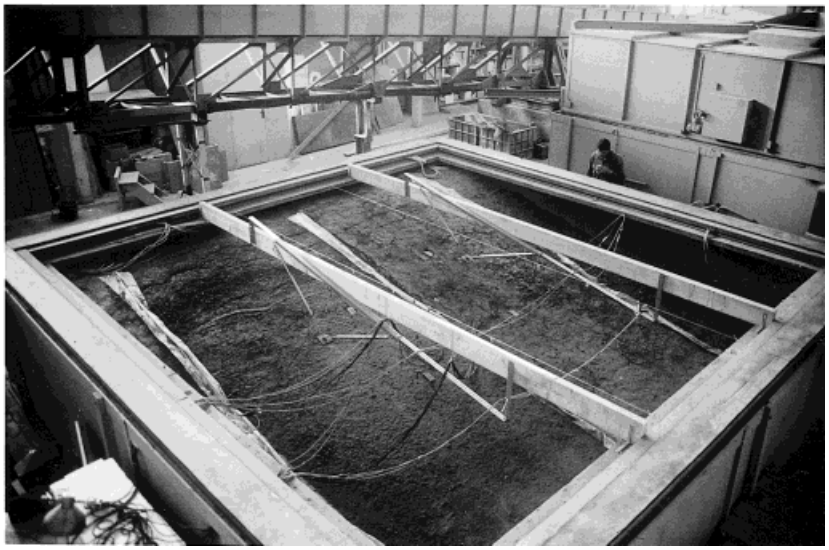

Figure 2. Experimental slope: lower left, Vire soil; upper right, Feuguerolles soil. Uppermost tiles in the two Feuguerolles tile columns are visible below the LVDT support beam. Cables leading to PC logging system (out of shot) are visible bottom left.

Table I. Comparison between experimental soil properties and solifluction field sites

| Soil | Clay % | Silt % | Sand % | Gravel % | Liquid limit (%) | Plastic limit (%) | Plasticity index (%) | Bulk density ($kg\,m^{-3}$) | Dry Density ($kg\,m^{-3}$) |
|---|---|---|---|---|---|---|---|---|---|
| Experimental soil: Feuguerolles | 2 | 16 | 59 | 23 | 29 | 17 | 12 | 2034 | 1685 |
| Experimental soil: Vire | 3 | 39 | 42 | 16 | 31 | 18 | 13 | 1941 | 1535 |
| Okstindan, Norway (Harris, 1977) | 15 | 23 | 52 | 10 | 23 | 21 | 2 | 2048 | 1660 |
| Tasariaq, Greenland (Everett, 1967) | 2–6 | 35–40 | 60–62 | | 14–22 | 10–16 | 2–6 | | 1630 |
| Mesters Vig, Greenland (Washburn, 1967) | | | | | 19–33 | 15–22 | 4–11 | | 1540–2140 |
| Canadian Rockies (Smith, 1992) | 5–28 | 21–56 | 45–69 | | 21–32 | 10–32 | 0–15 | 1000–1502 | |
| Banks Island, Canada (French, 1974) | Silty sand | | | | 17–32 | 10–23 | 7–9 | | |

embedded in the soil surface (Figures 1 and 2). As frost heaving of the surface occurred, followed by thaw settling and gelifluction, the change in length of the LVDTs was monitored, allowing the vectors of footplate movement to be calculated to an estimated accuracy of ±1·5 mm over a 20°C temperature range.

In addition, two columns of 80 mm × 40 mm × 10 mm unglazed ceramic tiles were installed in each soil, one upslope and the other downslope of the LVDTs (A,B,C,D in Figure 1). Columns were perpendicular to the slope surface and extended from the surface to the base of the experimental soils. The position of the uppermost tile in each of the buried columns was recorded manually against a benchmark at the beginning and end of each

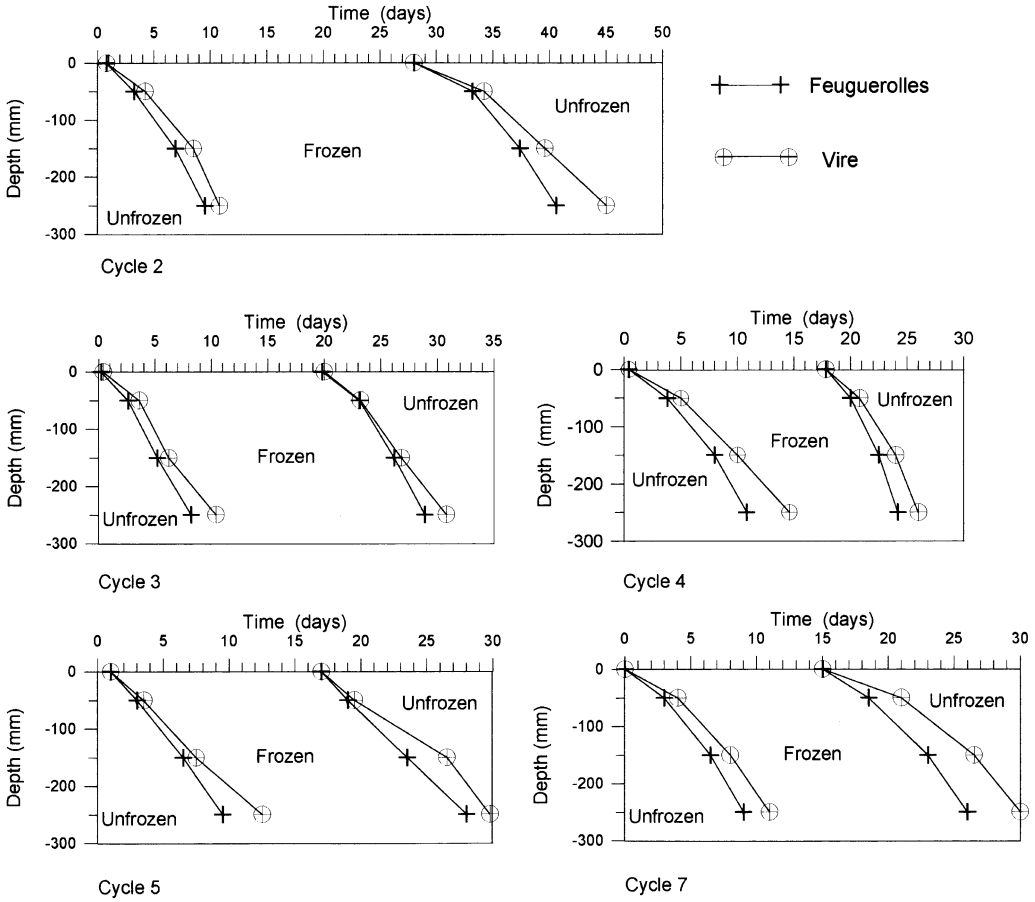


Figure 3. Zero degree isotherms: cycles 2 (January/February 1994), 3 (May/June 1994), 4 (July 1994), 5 (October 1994) and 7 (January/February 1995).

Table II. Soil thermal regime, frost heaving and surface downslope soil movements, Cycles 2 to 7. Downslope surface movements were measured manually and are the average of two surface markers on each soil, one above and one below the LVDT footplates

| Soil | Cycle no. | Mean freezing rate (mm hr$^{-1}$) | Total surface frost heave (mm) | Mean heaving ratio | Excess water content (% frozen volume) | Mean thaw rate (mm hr$^{-1}$) | Downslope surface soil movement (mm) |
|---|---|---|---|---|---|---|---|
| Feuguerolles | 2 | 1·13 | 57 | 0·160 | 14·37 | 0·83 | 23 |
| | 3 | 1·23 | 66·5 | 0·182 | 16·33 | 1·27 | 32 |
| | 4 | 1·04 | 65 | 0·178 | 16·03 | 1·58 | 36 |
| | 5 | 1·20 | 70 | 0·171 | 15·41 | 0·96 | 27 |
| | 6 | 1·39 | 53 | 0·150 | 13·50 | | 18 |
| | 7 | 1·16 | 59 | 0·164 | 14·76 | 0·95 | 28 |
| Vire | 2 | 0·96 | 78 | 0·206 | 18·57 | 0·61 | 100 |
| | 3 | 1·00 | 81 | 0·213 | 19·13 | 0·96 | 111 |
| | 4 | 0·72 | 90 | 0·232 | 20·77 | 1·20 | 169 |
| | 5 | 0·91 | 88 | 0·191 | 17·22 | 0·79 | 112 |
| | 6 | 1·15 | 64 | 0·176 | 15·84 | | 69 |
| | 7 | 0·93 | 77 | 0·204 | 18·36 | 0·69 | 77 |

freezing and thawing phase. The average value of surface displacement recorded by each of the two columns was taken as indicating surface movement for that soil in the midslope location.

During soil thawing, the LVDT triangle footplates remained frozen in place until the thaw plane had penetrated below 20 mm depth, so that downslope displacement of the upper 20 mm of soil was not detected by the LVDTs. Manual measurement of the ceramic tile columns at the end of each thaw cycle allowed this surficial soil movement to be quantified. The columns were excavated after seven complete freeze–thaw cycles to provide an independent check on the profiles of soil movement.

## RESULTS

### *Thermal regime*

Soil thermal regimes are illustrated in Figure 3, where zero-degree isotherms are plotted for the freezing and thawing periods of cycles 2–5 and cycle 7. Incomplete data sets are available for cycles 1 and 6. Rates of frost and thaw penetration were consistently lower in the Vire than in the Feuguerolles soil (Table II). This reflected the greater frost susceptibility of the former, which resulted in greater ice segregation, frost heaving and a higher excess ice content. Latent heat exchanges in the Vire soil therefore exceeded those in the Feuguerolles soil during both freezing and thawing periods.

### *Frost heave*

The downward penetration of the freezing front through each experimental soil resulted in progressive heave at the soil surface, detected by the LVDTs (Figure 4). Although the LVDT footplates were embedded to a depth of 20 mm, they became frozen into the soil surface, and successfully recorded heave in the upper 20 mm of soil. Comparison between frost heaving recorded by the LVDTs and that recorded manually showed no significant difference between the two methods. Total surface heave ranged from 53 to 70 mm in the Feuguerolles soil and from 64 to 90 mm in the Vire soil (Table II). In both experimental soils, heave rates were highest in the first few days of freezing. In cycle 4, for instance, rates of 5·75 mm/day were recorded during the first four days in the Feuguerolles soil and 9·4 mm/day during the first five days in the Vire soil (Figure 4).

Reference to the downward progress of frost penetration (Figure 3) and the corresponding progressive development of surface frost heaving (Figure 4) for each cycle and each soil enabled freezing cycles to be divided into periods with approximately constant heaving rates. By relating the beginning and end of these periods to recorded frost penetration depths, changes in heaving ratio during downward frost penetration were determined for each soil and each cycle. Results are illustrated in Figure 5. Clearly, heaving ratios (and hence excess ice contents) were consistently highest within the uppermost soil layers (maximum heaving ratio: Vire, 0·48 (cycle 4); Feuguerolles, 0·31 (cycle 7)). Heaving ratios also tended to increase near the interface between the experimental soils and the underlying sand layer, reflecting proximity to the basal water supply.

During each freezing cycle, frost penetration extended slightly below the bases of the experimental soils, into the underlying sand layer. The result was a rapid increase in frost heave rate at the end of each freezing cycle (Figure 4), suggesting that the interface between soil and sand became ice-rich. Since no temperature sensors were located within the basal sand layer it is impossible to assess the thickness of the basal frozen zone, but if basal soil frost penetration rates are projected downwards into the sand, heaving ratios of the order of 0·3 are indicated.

### *Thaw consolidation and downslope soil movement*

In their earlier slope simulation experiments, Harris *et al*. (1993) stressed the importance of frost heave and subsequent thaw consolidation in determining surface solifluction rates. These earlier experiments used similar slope geometry, hydraulic and thermal regimes to the present experiment, and included test slope sections of both the Vire and Feuguerolles soils. Harris *et al*. (1993) showed a linear relationship between surface frost heave and subsequent thaw-induced downslope surface displacement over 15 cycles of freezing and thawing, with the following regression equations:

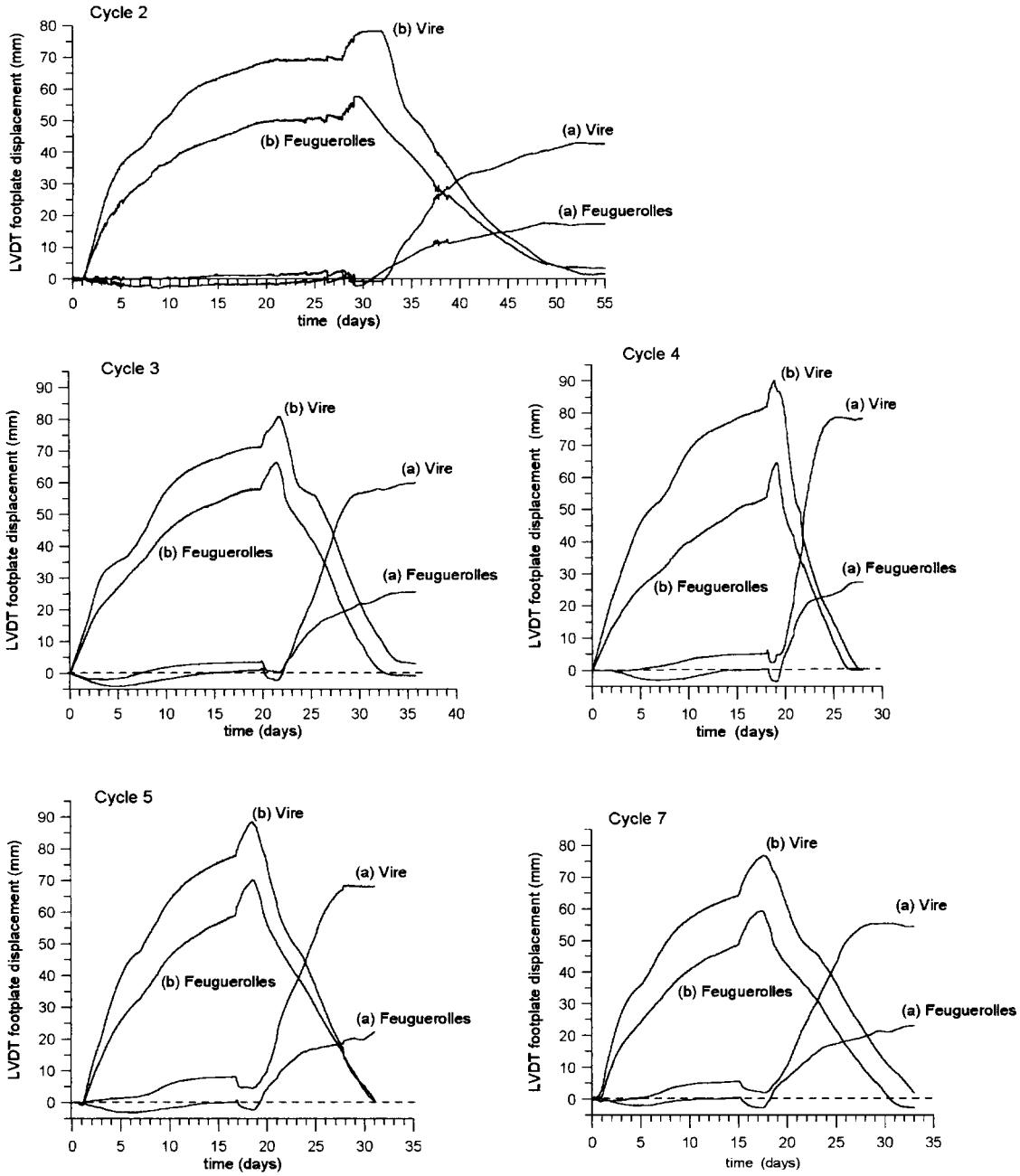


Figure 4. LVDT footplate displacements: (a) parallel to the soil surface (downslope displacement) and (b) perpendicular to the soil surface (heave/settlement). Note that no thaw settlement or downslope displacement was registered until thaw had penetrated to the base of the LVDT footplates (20 mm).

$$m = 0{\cdot}84h - 23{\cdot}12\ (r = 0{\cdot}89) \qquad \text{(Feuguerolles)}$$
$$m = 2{\cdot}19h - 65{\cdot}64\ (r = 0{\cdot}755) \qquad \text{(Vire)}$$

where $m$ = downslope soil movement at the surface and $h$ = surface frost heave (in millimetres).

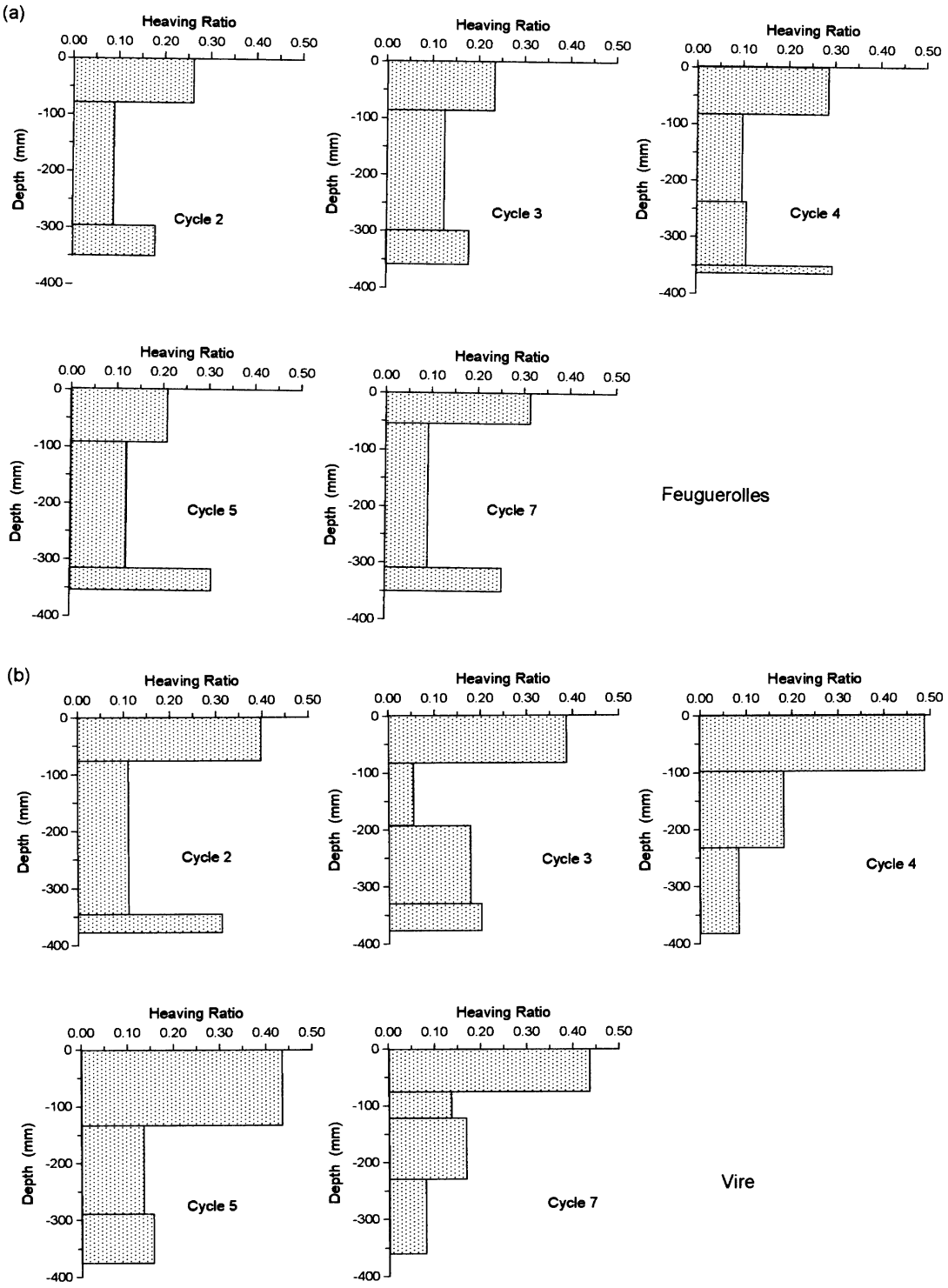


Figure 5. Heaving ratio (ratio of frost heaving/frozen soil thickness) profiles estimated from LVDT and thermal data: (a) Feuguerolles; (b) Vire.

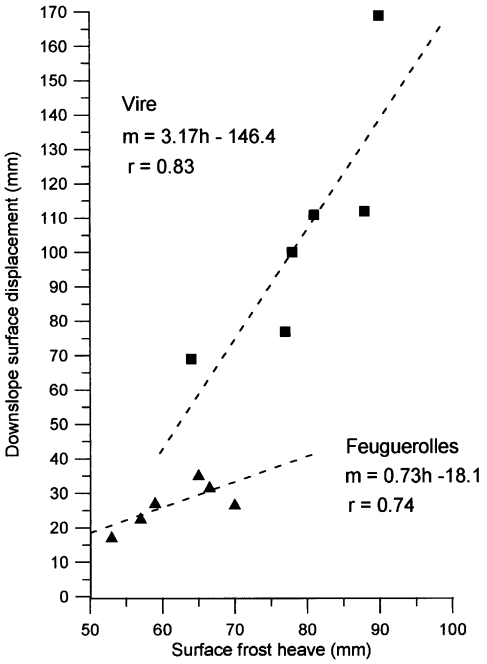


Figure 6. Scatter graphs and linear regression analysis of downslope surface soil movement against surface frost heave, cycles 2–7.

The present experiment also showed high correlation between frost heave measured by the LVDTs and downslope surface displacement measured manually (Figure 6), and similar regression equations:

$$m = 0{\cdot}73h - 18{\cdot}1 \ (r = 0{\cdot}74) \qquad \text{(Feuguerolles)}$$
$$m = 3{\cdot}17h - 146{\cdot}4 \ (r = 0{\cdot}83) \qquad \text{(Vire)}$$

Thus, it appears that the laboratory simulation experiment discussed in this paper is highly reproducible, giving consistent results that are dependent largely on soil characteristics.

Frost heave and resettlement perpendicular to the slope surface, and downslope soil movement parallel to the slope surface as recorded by displacements of the LVDT footplates are plotted against time in Figure 4. Reference to Figure 3 and Table II indicates that thaw penetration rates increased successively between cycles 2, 3 and 4. In response to this, rates of downslope soil displacement recorded by the LVDTs showed a parallel increase in both experimental soils. In cycles 5 and 7, rates of thaw and downslope displacement were intermediate to low. Only incomplete data sets are available for cycles 1 and 6. In the Feuguerolles soil, the rate of displacement was greatest during the first few days of thawing in all cycles, with soil movement rates tending to decrease later in each thaw phase (Figure 4). Maximum rates of downslope movement ranged from 1·44 mm/day in cycle 2 to 8·3 mm/day in cycle 4. In the Vire soil, apart from cycle 2, near-surface displacement rates remained roughly constant through each thaw period, with maximum rates ranging from 4·7 mm/day (cycle 2) to 14·8 mm/day (cycle 4).

Thaw settlement and downslope displacement data may also be presented as vectors of footplate movement (Figure 7a,b). The contrast between the two experimental soils, both in frost heaving during freezing and downslope soil displacement during thaw, is clearly demonstrated. A slight upslope displacement of the LVDT footplates during frost heaving was recorded, with a marked upslope displacement at the end of each freezing phase. The latter almost certainly reflects freezing of the soil/basal sand interface and back-tilting of the slope caused by greater frost heave at the foot of the slope where moisture contents were higher.

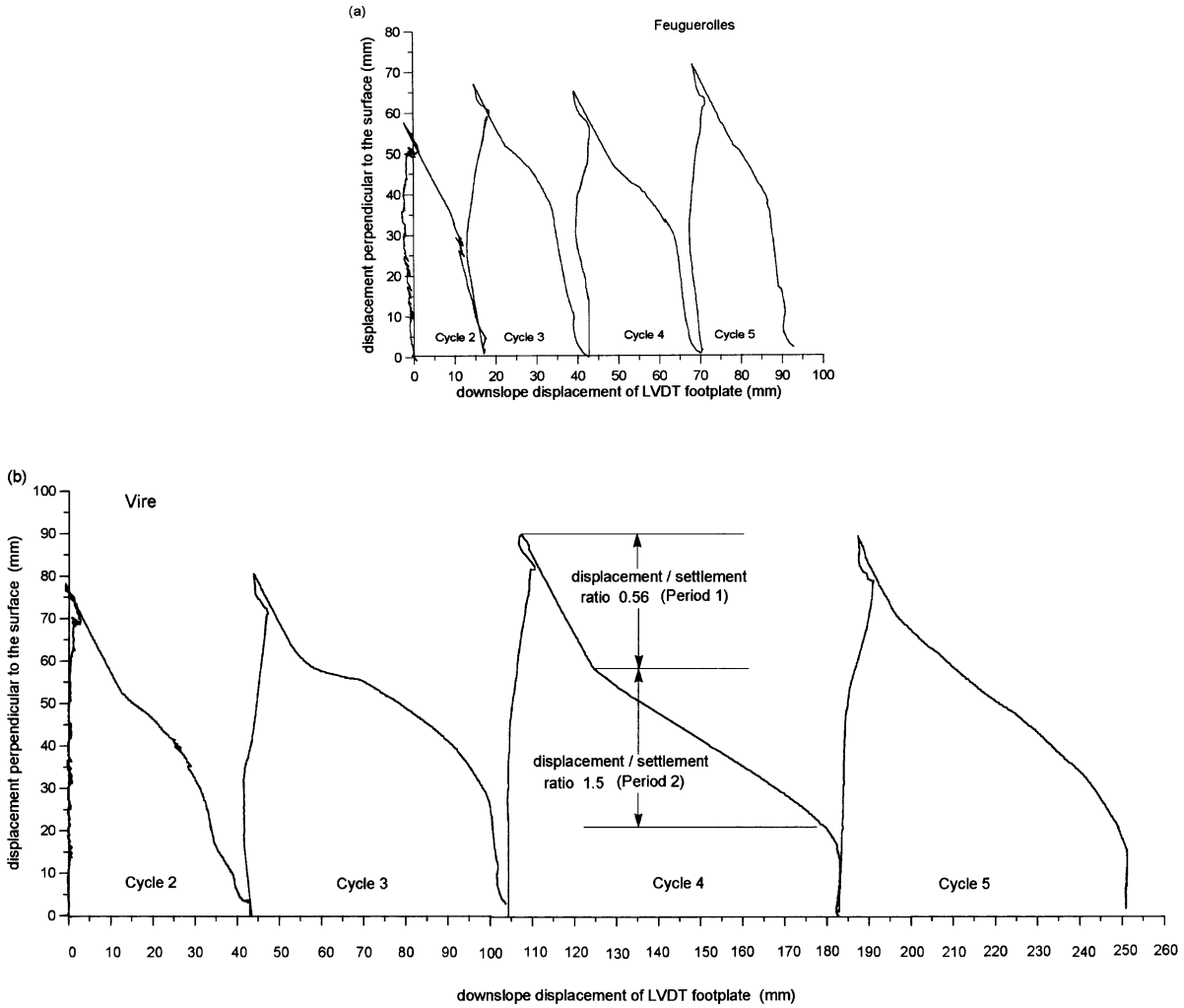


Figure 7. Vectors of surface soil movement during cycles 2, 3, 4 and 5: (a) Feuguerolles soil; (b) Vire soil. Note that displacements were measured with respect to a surface slope of 12°, so for true vectors, axes must be rotated clockwise by 12°. The LVDTs did not detect downslope thaw displacements in the uppermost 20 mm of soil, and therefore significantly underestimate total surface movement. Cycle 4 (Vire) demonstrates the procedure for determining profiles of soil displacement (see text).

*Profiles of soil shear strain*

Data collected during thawing of the experimental slope (Figures 3, 4 and 7) allow calculation of the distribution of soil shear strain with depth for each thaw period. These calculated displacement profiles are based on the assumption that strain within a given soil layer occurs during the period when that layer is thawing and consolidating, and ceases once thawing and thaw consolidation progress to the next layer down. Thus it is assumed that strain occurs at the thaw plane during thaw consolidation, and does not subsequently continue as deeper layers thaw.

Reconstruction of the profiles of soil shear strain may be most clearly illustrated with reference to the data for the Vire soil in cycle 4. Figure 7b shows that as thaw penetration extended below the base of the LVDT footplate (20 mm depth), thaw consolidation was registered with associated downslope displacement, the displacement/thaw settlement ratio being initially more or less constant at 0·56 (period 1, Figure 7b). The

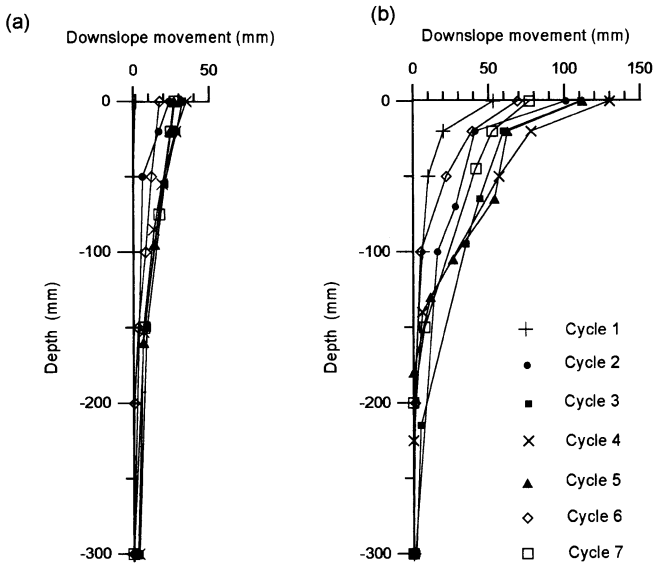


Figure 8. Profiles of downslope soil movement (soil shear strain) for each cycle calculated from LVDT and thermal data, plus manual measurement of surface tiles: (a) Feuguerolles; (b) Vire.

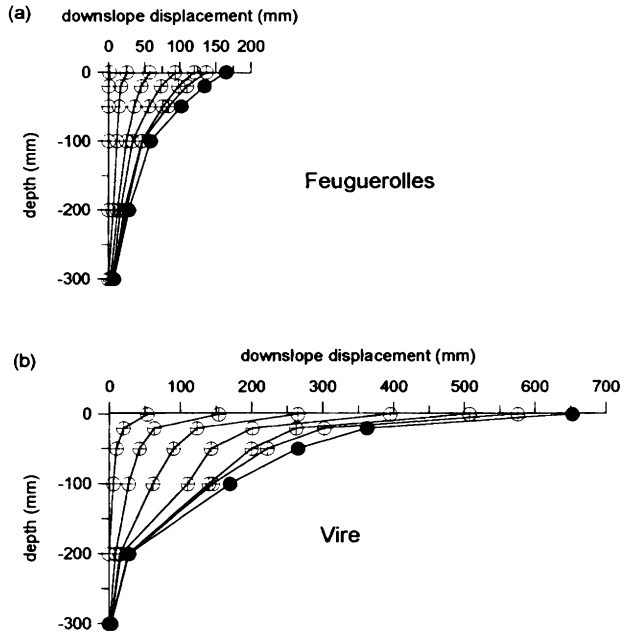


Figure 9. Accumulated profiles of downslope soil movement (soil shear strain), calculated from LVDT and thermal data, plus manual measurement of surface tiles: (a) Feuguerolles; (b) Vire.

displacement/thaw settlement ratio then changed sharply to a constant 1·5 (period 2, Figure 7b). The transition from period 1 to period 2 occurred when the surface had resettled by 32 mm. The soil settlement against time graph (Figure 4) shows this to have been 20·8 days after the beginning of cycle 4, and at this stage, thawing had

penetrated to a depth of 50 mm (Figure 3). Thus it may be assumed that LVDT footplate displacement over period 1 in Figure 7b reflected strain in the thawed soil over a depth range from 20 mm (when footplate displacement began) to 50 mm (the end of period 1 in Figure 7b). The differential downslope displacement over this 30 mm thick layer was therefore 17 mm. Similar calculations throughout the thaw phase, relating displacement to settlement to time to thaw depth, allowed the profile of soil displacement below 20 mm depth to be constructed.

The LVDT data exclude displacement of the uppermost 20 mm of soil, which occurred before the LVDT footplates thawed out, but manual measurement of the marker tiles allowed the differential movement between the soil surface and 20 mm depth to be quantified and a complete profile of soil movement to be determined for each soil in each cycle (Figure 8). The accumulated soil shear strain was then determined through addition of successive displacement profiles (Figure 9). In both soils, the profiles of movement are strongly concave downslope, and resemble field movement measurements where the surface is not bound with vegetation. At the end of the experiment, following seven cycles of freezing and thawing, the estimated midslope total downslope surface displacements amounted to 653 mm for the Vire soil and 165 mm for the Feuguerolles soil.

Excavation of the buried tile columns at the end of the seven cycles of soil freezing and thawing allowed the profiles of accumulated soil strain to be determined (Figure 10a,b). Profiles strongly resemble those reported by Harris *et al*. (1993), with both soils displaying greatest strain at around 50 mm depth. A comparison between the observed and predicted profiles of soil movement (Figure 11) indicates that the assumption made in calculating the distribution of shear strain with depth from the LVDT data (shear strain within a given soil layer occurs only while it is thawing and consolidating and ceases once thawing and consolidation has moved to a lower layer) results in an overestimation of downslope soil displacements at depth, and an underestimation of the displacement near the surface. It appears, therefore, that the viscosity of the thawing soil in the upper parts of the profiles remained sufficiently low for strain to continue after these layers had consolidated following thaw. Possible causes for prolongation of strain in the near-surface soil layers beyond their main period of thaw consolidation are considered below.

*Porewater pressure and hydraulic gradient during thaw*

Three porewater pressure transducers were installed in the Vire soil at depths of 50, 150 and 250 mm, and two in the Feuguerolles soil, at 50 mm and 250 mm depth. Transducers recorded negative pressures (tensions) during the period of thaw (the thermal 'zero curtain'), but pressures rose rapidly and were positive immediately following thaw, falling slowly over the next few days. Typical examples of porewater pressure changes are illustrated in Figures 12 and 13. Pore pressure data were used by Harris *et al*. (1995) in an effective stress analysis of thaw slope stability based on the infinite slope model, and apart from pore pressures recorded at 250 mm during cycle 3, calculated factors of safety ($F_s$) were greater than unity, indicating that the slope remained stable from rapid landsliding. The one exception ($F_s$ = 0·88) did not induce slope failure, the supercritical porewater pressures possibly being localized and caused by an area of high ice content.

Of particular interest in the present context is the relationship between measured pore pressures through the soil profiles as they thawed. Since thawing progressed downwards and peak porewater pressures at any given depth occurred for a short time immediately after thawing at that depth, an upward hydraulic gradient in excess of hydrostatic prevailed above the thaw plane (Figures 12 and 13). Thus, water movement during thaw was upwards, away from the thaw plane, towards the surface. This upward seepage of water would have had two effects: firstly, seepage pressures would have lowered effective stress between soil grains, reducing the frictional strength of the soil; and secondly, seepage would have maintained high soil moisture contents in the upper soil layers over a prolonged period by supplying water from below, thereby helping to maintain low values of viscosity in the near-surface soil and enhancing near-surface shear strain under downslope gravitational stress.

Thus, these data suggest that solifluction, the pre-failure straining of thawing soils, takes place due to reduced intergranular friction associated initially with consolidation-induced raised porewater pressures and subsequently with upward seepage pressures. Since shear strengths are not exceeded by gravitational stresses (i.e. rapid translational slope failure does not occur), the stress–strain relationships of the wet thawing soils may be defined by the soil viscosity. Such subcritical stress–strain relationships are almost certainly specific to each

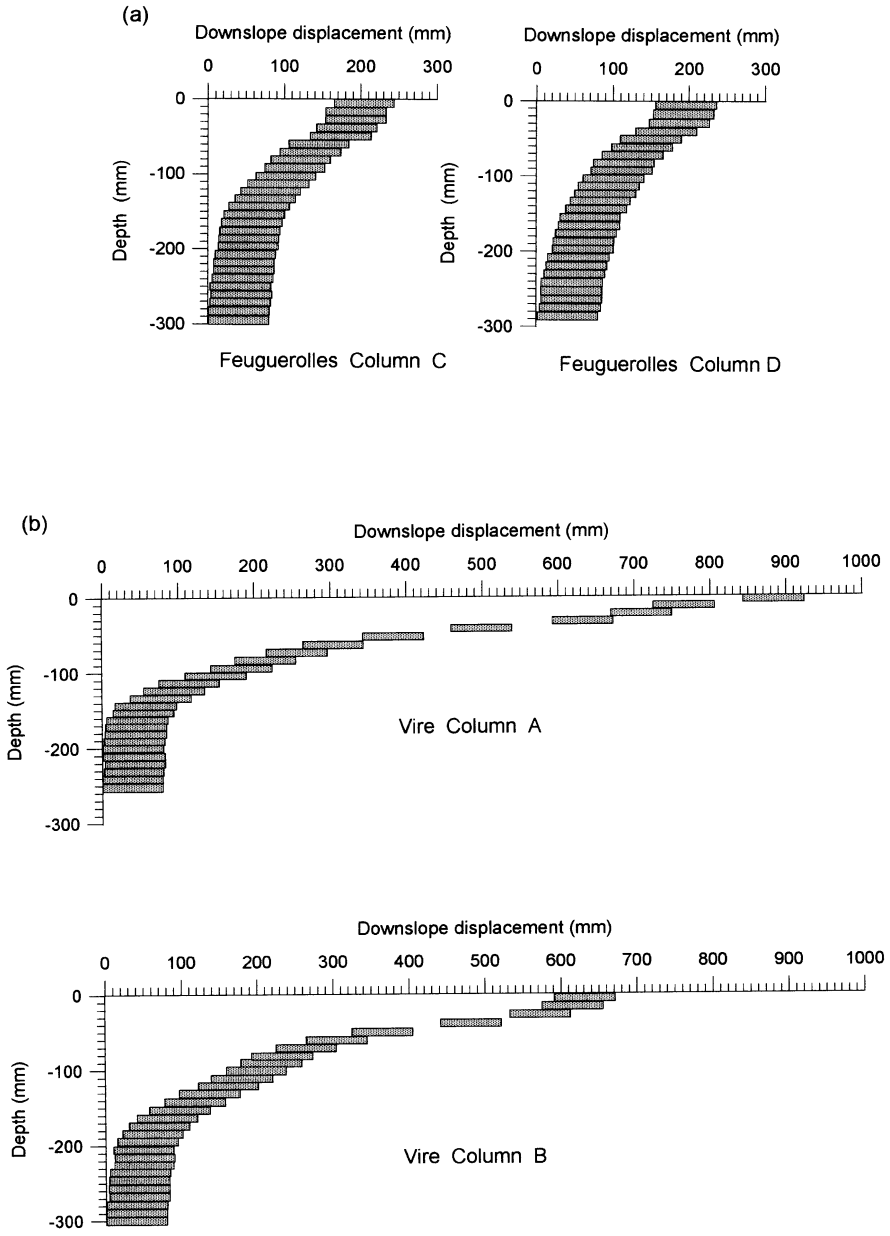


Figure 10. Profiles of soil movement after seven cycles revealed by excavation of tile columns: (a) Feuguerolles; (b) Vire.

soil and determined in part by the moisture content. In order to explore the possibility of quantifying moisture content–viscosity relationships, preliminary investigations were undertaken using the Carrimed 100 Controlled Stress Rheometer. Results are presented below.

*Rheology of the experimental soils*

Approximately 500 g samples of each experimental soil were air-dried and passed through a 425 μm sieve to remove the coarse sand and gravel fractions, following the British standard pre-preparation of soil for the

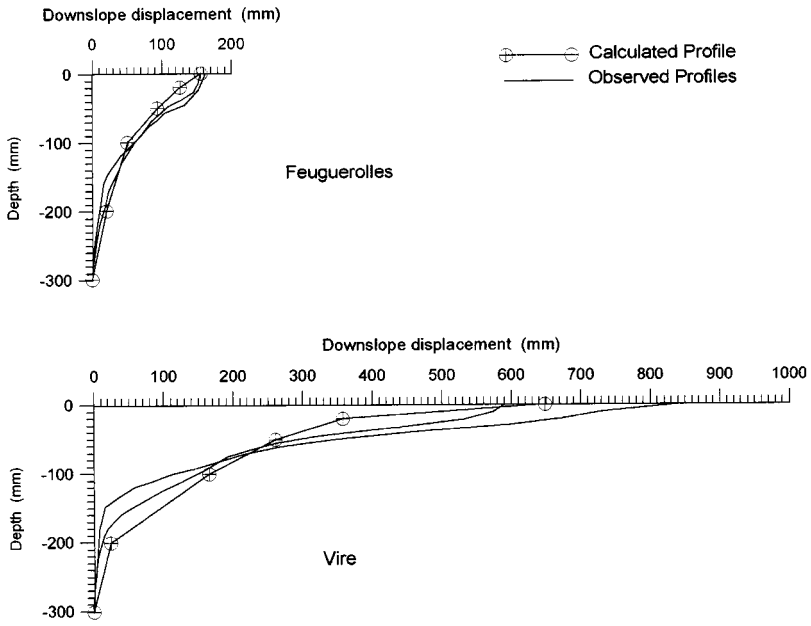


Figure 11. Comparison between displacement profiles estimated from LVDT and thermal data and profiles revealed by excavated columns.

Atterberg Limits test (British Standards Institution, 1990). Four hundred grams of each sample were then weighed and an appropriate amount of distilled water added to produce a moisture content of approximately 25 per cent by weight. Samples were thoroughly mixed in a food mixer for a period of 3 min. A subsample of each soil was placed in a parallel-sided beaker of diameter 50 mm. The beaker and sample were then placed on a vibrating table for 5 min, or until air bubbles ceased to be expelled at the soil surface. Rheometer tests were then made, using the Carrimed 100 Controlled Stress Rheometer with a 15 mm vane. The rheometer measures the stress–strain relationship for the specimen by determining the speed of vane rotation under progressively higher stress (vane torque) until the soil fails and rapid vane rotation takes place. Moisture content was determined following rheometer testing by oven-drying 10 g of each test sample at 110°C. The remaining test sample was remixed with the whole sample and sufficient water added to raise the moisture content by approximately 2 per cent. The procedure was then repeated over a moisture range from approximately 25 to 40 per cent. Two separate test series were undertaken for each soil to confirm reproducibility of results, and the combined data are plotted in Figure 14.

These curves clearly demonstrate that as soil moisture contents increase, viscosity (the ratio of shear stress/strain rate) decreases, so it is likely that the zone of maximum soil shear strain measured during the solifluction simulation experiment (20–100 mm depth, Figure 10) corresponded with the zone of highest moisture contents that persisted over the longest period of time. Monitoring during cycle 4 showed moisture contents in excess of the liquid limit (liquidity index >1) at a depth of 50 mm for a period of five days following passage of the thaw front in the Vire soil, and around two and a half days following passage of the thaw front in the Feuguerolles soil (Harris *et al.*, 1995). This was also the wettest part of the thawing profile. Cycle 4 moisture contents immediately above the thaw plane in the Feuguerolles soil were 29·5 per cent at 75 mm depth on day 3 of the thaw period, 26·4 per cent at 150 mm depth on day 5, and 25·5 per cent at 200 mm depth on day 6 of the thaw, and in the Vire soil, 37·5 per cent at 50 mm depth on day 3, 34·2 per cent at 100 mm depth on day 5 and 30·8 per cent at 180 mm depth on day 7. It is noteworthy that the LVDT frost heave data indicate that excess ice contents in the frozen soil profiles were consistently highest in the uppermost soil layers (Figure 5a,b).

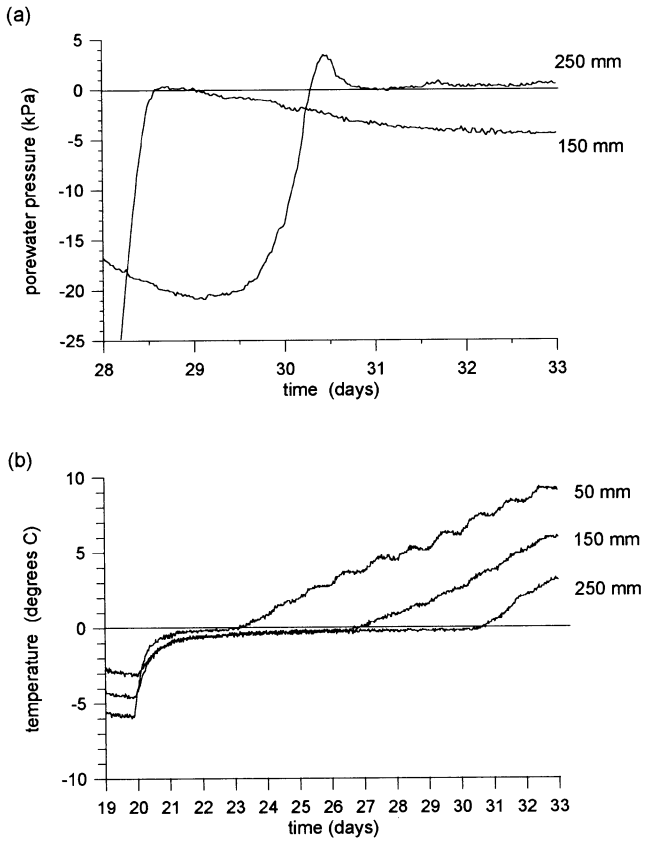


Figure 12. Porewater pressures and soil temperatures, Vire soil: (a) porewater pressures, cycle 3; (b) temperatures, cycle 3.

Undrained shear strength (yield stress) measurements using a hand shear vane, together with determinations of corresponding soil moisture contents, were made on the experimental slope as thawing progressed during cycle 4 (Harris *et al.*, 1995). Plots of log yield stress (undrained shear strength) against liquidity index (moisture content minus plastic limit divided by plasticity index) and moisture content for the hand shear vane determinations, together with the subsequent laboratory rheometer measurements, show consistent relationships (Figure 15a,b), suggesting that the rheometer tests were undertaken with soil properties representative of the experimental thaw periods. The rheometer data show little scatter and plot close to the lower boundary of the hand vane data, reflecting the much greater precision of the rheometer. The scatter of points in the hand shear vane data probably reflects errors in soil moisture content determination due to water entering the small trial pits excavated for gravimetric sampling.

Comparison between yield stress and moisture content in the two soils (Figure 14) shows that, for a given moisture content, the sandier Feuguerolles soil is softer, with a lower yield stress than the Vire soil. Despite this, recorded shear strain was much greater in the Vire soil (Figures 10 and 11) than the Feuguerolles soil. Regression analysis of surface movement against frost heave also showed much lower surface movement rates for a given amount of heave in the Feuguerolles soil than in the Vire soil (Figure 6). These differences in susceptibility to solifluction relate to the lower frost susceptibility and higher permeability of the sandier Feuguerolles soil, resulting in lower moisture contents and more rapid drainage during soil thawing. The relationships between stress and strain rate for different moisture contents illustrated in Figure 14 provide the

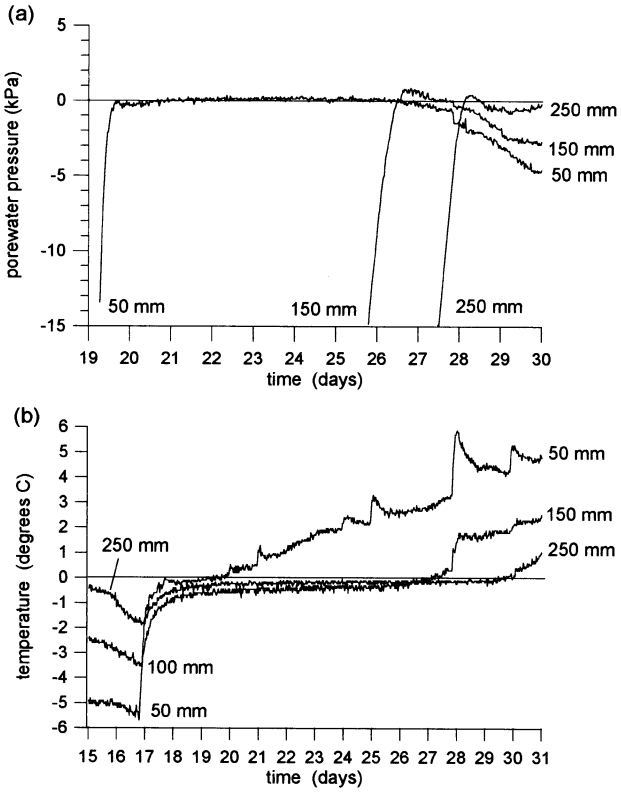


Figure 13. Porewater pressures and soil temperatures, Vire soil: (a) porewater pressures, cycle 5; (b) temperatures, cycle 5.

opportunity for future quantitative modelling of solifluction in these two soil types, utilizing knowledge of excess ice content, thaw rate and post-thaw changes in moisture content.

## DISCUSSION AND CONCLUSIONS

The experiments described in this paper have enabled detailed monitoring of frost heave, resettlement and downslope displacements using LVDTs and this has demonstrated the importance of thaw settlement in causing downslope soil movements. By relating surface heave and resettlement to soil thermal data, the significance of the distribution of soil ice prior to the initiation of thaw has been explicitly shown. The high correlation between frost heave and total surface downslope displacement demonstrated in earlier studies has also been confirmed here.

Profiles of soil movement resemble those measured in field studies from many periglacial mountains, and if each monthly freeze–thaw cycle is considered to be equivalent to the annual field cycle of freezing and thawing, simulated rates of movement are similar to those reported in field studies.

Thaw consolidation causes raised but subcritical porewater pressures, and upward water seepage in response to an upward hydraulic gradient also generates seepage pressures. Both porewater pressures and seepage pressures reduce intergranular friction within the soil mass. Upward seepage also maintains higher soil moisture contents in the near-surface soil layers, thereby maintaining lower viscosities and promoting soil shear strain in response to the applied gravitational stress field. It has been demonstrated that soil shear strain in the upper soil layers may continue over several days after the soil has thawed, due to high soil moisture contents maintained by upward seepage of water expelled during thaw consolidation at depth.

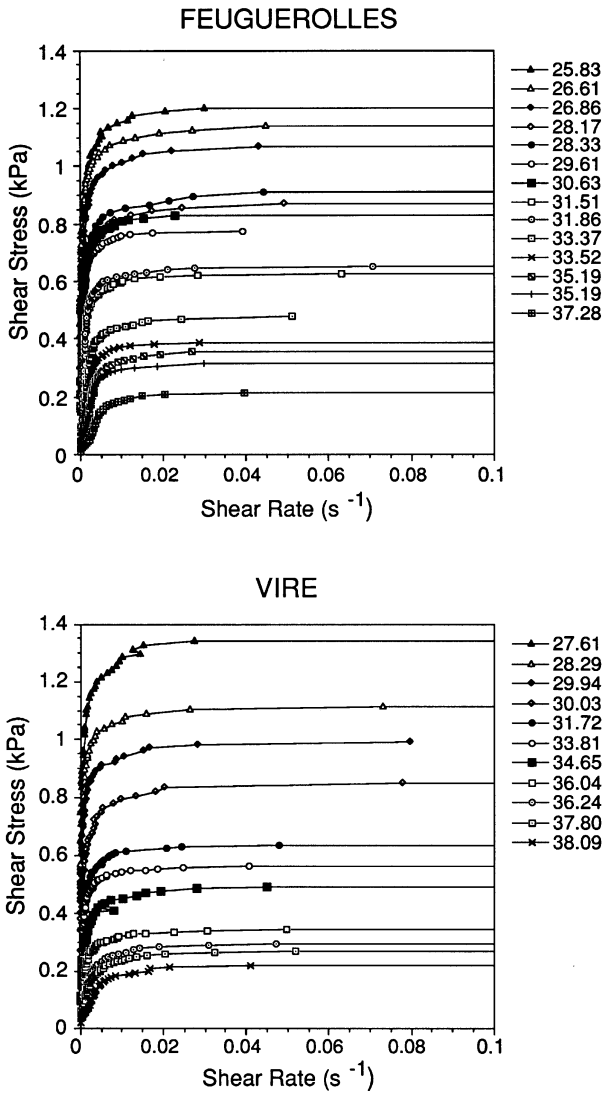


Figure 14. Stress – strain rate plots from Carrimed 100 Controlled Stress Rheometer for Feuguerolles and Vire soil samples at moisture contents between 25 and 40 percent. Numbers shown in the key are soil moisture contents expressed as percentage dry weight.

Testing with the Carrimed 100 Controlled Stress Rheometer indicated similar viscosity/moisture content relationships in the two soil types used here. Observed contrasts in the rates of solifluction recorded under identical thermal and hydraulic conditions reflect mainly the lower frost susceptibility and higher permeability of the sandy Feuguerolles soil than the more silt-rich (finer grained) Vire soil. As a result, the Feuguerolles soil showed significantly lower amounts of frost heave during freezing, and lower moisture contents and more rapid soil drainage following thaw than the Vire soil. Soil viscosity has been shown to fall as moisture contents rise, and consequently the amount of shear strain observed during thaw of the Vire slope greatly exceeded that of the Feuguerolles slope. Moisture contents were higher and the soil remained wetter for longer in the former than in the latter. The derivation of viscosity/moisture content data offers the prospect of predicting soil strains during thawing of these soils under a range of soil thermal and moisture conditions, and this will form the next stage in this research.

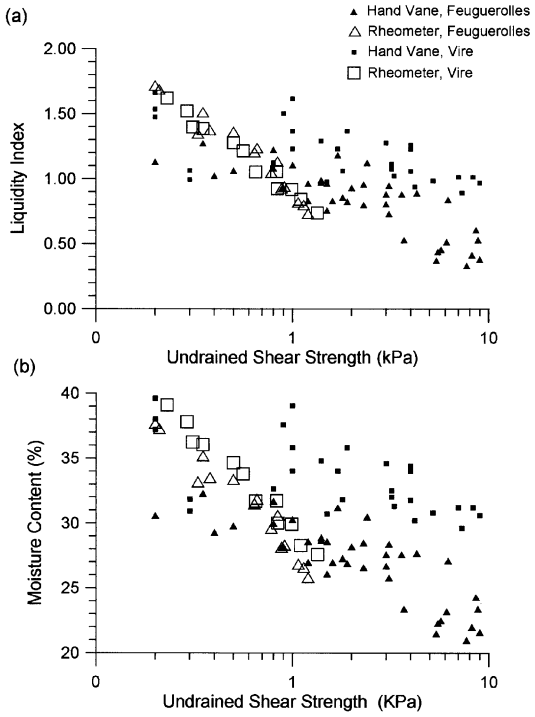


Figure 15. (a) Scatter graph of undrained shear strength against liquidity index during the thaw period of cycle 4 measured with hand shear vane, together with laboratory rheometer yield stress values against liquidity index. (b) Scatter graph of undrained shear strength against moisture content during the thaw period of cycle 4 measured with a hand shear vane, together with laboratory rheometer yield stress values against moisture content.

The experimental procedure described in this paper involved full-scale physical modelling of slope processes associated with downward freezing and thawing of silty soils. Field equivalents are considered to be those areas with deep seasonal frost penetration, or warm permafrost, where only one-sided (surface downward) soil freezing is significant. Such areas include the European Alps, the Scandinavian mountains, the Rocky Mountains of North America and many sub-arctic areas. In the field, snowmelt may supply moisture to the soil and maintain wet conditions for a longer period than in the simulation experiments. During thaw consolidation, however, an upward hydraulic gradient within a thawing soil would prevent the entry of surface snowmelt. Field studies in Okstindan, North Norway, by Harris (1972, 1977) showed melting snow supplying surface runoff across a monitored solifluction slope. At this location, an attempt was made to introduce fluorescent dye into the thawing soil via a surface trench, in order to trace water movement paths. Subsequent soil sampling showed that no dye had entered the soil, probably due to the presence of an upward hydraulic gradient and associated upward soil water seepage similar to that observed in the experimental simulations described in this paper.

Where cold permafrost is present and two-sided freezing of the active layer takes place, the distribution of soil ice at the beginning of the thaw phase would be different from that simulated in the cold room experiments described here, resulting in the zone of maximum shear being located at a different depth in the soil profile. High ice contents near the base of the active layer are reported in many areas with continuous permafrost and two-sided freezing of the active layer (e.g. Mackay 1981, 1983; Lewkowicz, 1992; Harris and Lewkowicz, 1993). Under these circumstances, the present laboratory simulation experiments suggest that pre-failure soil strain would be greatest in the basal ice-rich layer, resulting in plug-like solifluction movements as described by Mackay (1981) in the Mackenzie Delta of Canada. The processes responsible for thaw-induced soil strain observed during slope simulation experiments are considered likely to occur whenever ice-rich soils thaw. It is the distribution of soil ice within the profile that may vary between different periglacial environments, and this

determines the depth within the active layer at which thaw consolidation, moisture contents and soil strains are all maximum. Thus, although the profiles of soil movement reported here are directly applicable to surface-downwards soil freezing and thawing, the thaw-related processes described are considered to have a much wider significance. Simulation experiments to investigate solifluction rates and processes associated with two-sided freezing of the active layer will be undertaken at a later stage in this research.

## ACKNOWLEDGEMENTS

The authors gratefully acknowledge technical assistance from Mr Gerard Guillemet and Mr Derek John, and advice on rheometer testing from Dr John Roberts. Financial support from NERC (Research Grant GR9/1089), the University of Wales, Cardiff and the CNRS (France) is gratefully acknowledged.

## REFERENCES

Åkerman, H. J. 1993. 'Solifluction and creep rates 1972–1991, Kapp Linne, West Spitsbergen', in Frenzel, B. (Ed.), *Solifluction and Climatic Variation in the Holocene*, European Science Foundation, Stuttgart, 225–250.

Andersson, R. G. 1906. 'Solifluction, a component of subaerial denudation', *Journal of Geology*, **14**, 91–112.

Benedict, J. B. 1970. 'Downslope soil movement in a Colorado Alpine region: rates, processes and climatic significance', *Arctic and Alpine Research*, **2**, 165–226.

Bertran, P. 1993. 'Deformation-induced microstructures in soils affected by mass movements', *Earth Surface Processes and Landforms*, **18**, 645–660.

British Standards Institution, 1990. BS1377: *Methods of test for soils for civil engineering purposes*, British Standards Institution.

Coutard, J-P., Van Vliet-Lanoë, B. and Auzet, A. V. 1988. 'Frost heaving and frost creep on an experimental slope: results for soil structures and sorted stripes', *Zeitschrift für Geomorphologie, Supplementband*, **71**, 13–23.

Everett, D. H. 1967. 'Mass wasting in the Taseriaq area, West Greenland', *Meddelser om Grönland*, **165**, 1–32.

French, H. M. 1974. 'Mass-wasting at Sachs Harbour, Banks Island, N.W.T. Canada', *Arctic and Alpine Research*, **6**, 71–78.

French, H. M. 1976. *The Periglacial Environment*, Longman, London, 309pp.

Frenzel, B. 1993. *Solifluction and Climatic Variation in the Holocene*, European Science Foundation, Stuttgart, 387pp.

Harris, C. 1972. 'Processes of soil movement in turf-banked solifluction lobes, Okstindan, northern Norway', in Price, R. J. and Sugden, D. E. (Eds), *Polar Geomorphology*, Institute of British Geographers Special Publication **4**, 155–174.

Harris, C. 1977. 'Engineering properties, groundwater conditions, and the nature of soil movement on a solifluction slope in North Norway', *Quarterly Journal of Engineering Geology*, **10**, 27–43.

Harris, C. 1981. *Periglacial Mass Wasting: A Review of Research*, BGRG Research Monograph **4**, GeoAbstracts, Norwich, 204pp.

Harris, C. 1987. 'Mechanisms of mass movement in periglacial environments', in Anderson, M. G. and Richards, K. S. (Eds), *Slope Stability*, Wiley, Chichester, 531–559.

Harris, C. 1993. 'The role of climate and soil properties in periglacial solifluction: evidence from laboratory simulation studies', in Frenzel, B. (Ed.), *Solifluction and Climatic Variation in the Holocene*, European Science Foundation, Stuttgart, 295–308.

Harris, C. and Lewkowicz, A. G. 1993. 'Micromorphological investigations of active-layer detachment slides, Ellesmere Island, Canadian Arctic. *Proceedings of 6th International Permafrost Conference*, Beijing, China, S. China University of Technology Press, 232–237.

Harris, C., Gallop, M. and Coutard, J-P. 1993. 'Physical modelling of gelifluction and frost creep: some results of a large-scale laboratory experiment', *Earth Surface Processes and Landforms*, **18**, 383–398.

Harris, C., Davies, M. C. R. and Coutard, J-P. 1995. 'Laboratory simulation of periglacial solifluction: significance of porewater pressures, moisture contents and undrained shear strengths during soil thawing', *Permafrost and Periglacial Processes*, **7**, 293–312.

Harris, C., Davies, M. C. R. and Coutard, J-P. 1996. 'An experimental design for laboratory simulation of periglacial solifluction processes', *Earth Surface Processes and Landforms*, **21**, 67–76.

Higashi, A. and Corte, A. E. 1971. 'Solifluction: a model experiment', *Science*, **171**, 480–482.

Jahn, A. 1961. 'Quantitative analysis of some periglacial processes in Spitzbergen', *Universitet Wroclawski in Boleslawa Bieruta, Zezvytynankowe, Nanki Przyrodnicze Ser B*, **5**, 1–34.

Lewkowicz, A. G. 1988. 'Slope processes', in Clark, M. J. (Ed.), *Advances in Periglacial Geomorphology*, Wiley, Chichester, 325–370.

Lewkowicz, A. G. 1992. 'Factors influencing the distribution and initiation of active layer detachment slides on Ellesmere Island, Arctic Canada, in Dixon, J. C. and Abrahams, A. D. (Eds), *Periglacial Geomorphology*, Wiley, Chichester, 223–250.

Mackay, J. R. 1981. 'Active layer slope movement in a continuous permafrost environment, Garry Island, Northwest Territories, Canada', *Canadian Journal of Earth Sciences*, **18**, 1666–1680.

Mackay, J. R. 1983. 'Downward water movement into frozen ground, western arctic coast, Canada', *Canadian Journal of Earth Sciences*, **20**, 120–134.

Matsuoka, N. 1994. 'Continuous recording of frost heave and creep on a Japanese Alpine slope', *Arctic and Alpine Research*, **26**, 245–254.

Morgenstern, N. R. and Nixon, J. F. 1971. 'One-dimensional consolidation of thawing soils', *Canadian Geotechnical Journal*, **11**, 447–469.

Permafrost Subcommittee, National Research Council of Canada, 1988. *Glossary of Permafrost and Related Ground-ice Terms*, National Research Council of Canada Technical Memorandum No. **142**, 156pp.

Sigafoos, R. S. and Hopkins, D. M. 1952. *Soil stability on slopes in regions of perennially frozen ground*, Highway Research Board Special Report **2**, 176–192.
Smith, D. J. 1988. 'Rates and controls of soil movement on a solifluction slope in the Mount Rae area, southern Canadian Rocky Mountains', *Zeitschrift für Geomorphologie, Supplementband*, **71**, 25–44.
Smith, D. J. 1992. 'Long-term rates of contemporary solifluction activity in the Canadian Rocky Mountains', in Dixon, J. and Abrahams, A. (Eds), *Periglacial Geomorphology*, Wiley, Chichester, 203–221.
Taber, S. 1943. 'Perennially frozen ground in Alaska: its origin and history', *Bulletin of the Geological Society of America*, **54**, 1433–1548.
Van Vliet-Lanoë, B. 1985a. 'Frost effects in soils', in Boardman, J. (Ed.), *Soils and Quaternary Landscape Evolution*, Wiley, Chichester, 115–156.
Van Vliet-Lanoë, B. 1985b. 'From frost to solifluction: a new approach based on micromorphology, its application to arctic environment', *Inter Nord*, **17**, 15–20.
Van Vliet-Lanoë, B., Coutard, J-P. and Pissart, A. 1984. 'Structures caused by repeated freezing and thawing in various loamy sediments. A comparison of active, fossil and experimental data', *Earth Surface Processes and Landforms*, **9**, 553–566.
Washburn, A. L. 1967. 'Instrumental observations of mass-wasting in the Mesters Vig district, N.E. Greenland,' *Meddeleser om Grönland*, **166**, 1–297.
Williams, P. J. 1957. 'Some investigations into solifluction features in Norway', *Geographical Journal*, **123**, 42–58.